ENCLOSURE (1)

N8110R:72-033

ENGINEERING OPERATIONS REPORT

Verror
DRA

CHILLDOWN STUDY OF THE SINGLE STAGE INDUCER TEST RIG

PROJECT 110

2 JUNE 1972

L. A. KIMURA

L. A. Kimura

CLASSIFICATION CATEGORY
Unclassified
WR Thompson 5-17-72
CLASSIFYING OFFICER DATE

APPROVED:

for WR Thompson
U. A. PINEDA, MANAGER
APPLIED MECHANICS
ENGINEERING STAFF DEPARTMENT

L. A. Kimura
2 June 1972

CHILLDOWN STUDY OF THE SINGLE STAGE INDUCER TEST RIG

I. INTRODUCTION

The objective of the pump chilldown test was to obtain data which could be used for improving the pump analytical model and to observe phenomena which could influence pump chilldown.

The pump chilldown tests were conducted at NRDS (Nuclear Rocket Development Station) on a low priority basis in conjunction with the primary pump performance tests. These tests were performed in Test Cell "C" between December 8 and 22, 1971.

II. SUMMARY/CONCLUSIONS

Of the six chilldown tests, data from only one could be used for evaluation. During the rest of the chilldown tests, there was leakage hydrogen flow into the pump cavity prior to the initiation of the chilldown test. Prior to the test, it was hoped that two-phase flow data could be obtained from these tests. In all of the tests, however, the hydrogen condition into the pump was probably 100% vapor. The data from this one test, therefore, can be used to compare only the single phase fluid correlation in the analytical pump chilldown model.

All of the pump instrumentation and plumbing were based on the requirements of the single stage pump performance and cavitation experiments. The chilldown test was incorporated on a low priority basis without hardware modification nor additional instrumentation.

In general, the actual pump chilled down much faster than predicted by the analytical pump model. There were insufficient data from the test to measure the pump flow rate and pump inlet fluid condition; therefore, these parameters were extrapolated based on related data which were available. However, even with the highest probable flow rate, the pump chilled faster than predicted.

The pump metal temperature sensor is not located in an ideal place since there is a stagnant gas pocket between the sensor and the flowing coolant. In the analysis it was assumed that the gas between the impeller shroud and the

housing was trapped stagnant gas. The pump configuration is such that eddy currents can be set up in this pocket to enhance the heat transfer from the temperature sensor to the flowing coolant in the impeller. Other phenomena such as liquid carry-over in the gas and discontinuous flow at the impeller tip could lead to higher heat transfer coefficients than computed from a developed flow correlation.

Based on the experience gained from this series of chilldown tests, much can be learned about pump chilldown and ways of improving the analytical pump chilldown model. If further pump chilldown tests are performed with proper instrumentation and hardware modification, the recommendations are as follows:

1. The pump inlet flowmeter should be located upstream of the flow control valve; there then will be a better chance of maintaining 100% liquid in this flowmeter for accurate flow rate measurement.

2. Wide-range temperature readouts (35 to 500°R) are required for a chilldown test, not narrow range readouts (35-54°R).

3. The pump metal temperature sensors must be located adjacent to the fluid in an established flow regime in order to obtain good heat transfer data. The actual heat transfer coefficient may be several times larger near flow disruptions or entrance regions to a passage than in a fully developed flow region.

4. A better flow conditioner is required for pump chilldown tests. A temperature stratification of 70°R was measured in the pump inlet line only 20 in. downstream of the flow conditioner used in this test.

5. Since the two-phase convective heat transfer coefficient is probably the largest unknown in the pump chilldown analytical model, a serious attempt should be made to obtain two-phase flow data. To do so, the pump inlet line to the bypass line must be shortened as much as possible. Presently, this distance is approximately 14 ft.

III. DISCUSSION

A. PUMP CHILLDOWN TEST

1. General

Between December 8 and 22 in Test Cell "C" at NRDS (Nuclear Rocket Development Station), the liquid hydrogen pump component development

testing was conducted as described in the test plan (Reference 1). The pump chilldown tests were performed at the start of each testing day during the facility line chilldown phase. These chilldown tests were conducted on low priority, limited fund and tight schedule basis; therefore, instrumentations and piping modifications necessary for a more meaningful pump chilldown test could not be added to the system.

2. Test Description

It was originally anticipated that the pump chilldown test be conducted with 100% liquid hydrogen flowing through flowmeter KF-130 (see Figure 1) at approximately 1 lb/sec. Since the response characteristics of the total system were not known prior to testing, the first chilldown test was conducted primarily to learn the response characteristics and the limitations of the pump testing system as applicable to the pump chilldown tests.

Shown on Figure 1 is the Test Cell "C" piping and instrumentation diagram. In general, all the pump chilldown tests started with the facility line chilldown phase by-passing the pump (the following valves were closed: K-2, C-4, C-221). When KT-4 indicated liquid temperature, K-130 was opened and K-3 was closed to chill down flowmeter KF-130. When the facility line upstream of valve C-4 was completely chilled down, K-130 was closed to stop flow while valves to flare remained open to vent the down stream lines. When the boil-off rate became very small (CP-6 near ambient) C214 was closed and C-4 and K-130 were opened to initiate the pump chilldown test.

In the first chilldown test (performed on December 8), during the facility line chilldown phase, the pump was partly cooled down due to a leakage through either valve C-4 or check valve CC-1005 and venting through C-231 to flare. When the chilldown test was initiated, the flow reading at KF-130 was very erratic. Valve C-8 was partially closed to maintain back pressure in the loop down-stream of the pump to prevent over-speeding of flowmeter CF-6 with 100% vapor. Unfortunately, this back pressure left very little pressure differential across valve K-130 for controlling the flow rate through flowmeter KF-130.

For the 2nd test (performed on December 10), it was proposed that valve C-231 be closed during the facility line chilldown to prevent leakage flow through the pump from C-4 or C-1005 and thence out to flare. By closing valve C-231, even if there is a leak, once the pressure in the pump equals the line pressure, the leakage flow would stop. It was also recommended to leave valve C-8 wide open to allow valve K-130 sufficient pressure drop to control the flow rate through flowmeter KF-130. This second chilldown test proceeded smoothly with no pre-chilling of the pump prior to the initiation of the chilldown test and with smooth flow rate readings.

The following four chilldown tests (December 15, 16, 17 and 22) all experienced leakage flow into the pump prior to the initiation of the chilldown test and many of the temperature readouts of the pump were lost by then.

B. DATA ANALYSIS

1. Selection of Data for Analysis

In all six chilldowns, the fluid condition at the pump inlet flowmeter (KF-130) was two-phase hydrogen and at the outlet flowmeter (CF-6) was 100% hydrogen vapor. All of the chilldown tests except one experienced leakage flow through the pump which pre-chilled the pump prior to the actual initiation of the chilldown test. Since it is very difficult to evaluate the test data in which leakage flow occurred, data analysis was concentrated on the single chilldown test. Also, the later chilldown tests (December 17 and December 22) had lost most of the pump temperature sensors.

2. Measured Temperature Response

Shown on Figure 2 are the measured temperatures from the 2nd chilldown test (December 10). The locations of the temperature sensors and their readout range are shown on Table 1. The complete instrumentation specification for these tests are given in the test plan (Reference 1).

The pump metal temperatures were measured (Figure 3) near the front face of the impeller outlet at .2, .3 and .4 in. from the fluid (CT-700, CT-701 and CT-702 respectively). As expected, the temperature sensor nearest the

fluid chilled down the fastest and the sensor farthest from the fluid was the slowest. The bearing fluid temperature (CT-703) chilled down with the pump metal temperature and towards the end of the chilldown test was colder than the metal temperatures.

3. Fluid Flow Rate

The hydrogen flow rate through the pump was measured by KF-130 located in the line approximately 60 ft upstream of the pump inlet and by CF-6 located in the line approximately 24 feet downstream of the pump outlet. Prior to the chilldown test, it was anticipated that 100% liquid could be maintained in the upstream flowmeter (KF-130); but, due to the low flow rate (approximately 1 lb/sec) and the location of the flow control valve in respect to the flowmeter, two-phase fluid flowed through this flowmeter. If the flow control valve was located downstream of the flowmeter so that the flowmeter is on the higher pressure side of the control valve, 100% liquid could probably have been maintained in the flowmeter during the chilldown tests.

All during the chilldown test, the fluid condition was always 100% vapor at the pump outlet flowmeter, CF-6. By using the perfect gas laws, the measured volumetric flow rate can be converted to mass flow rate. The fluid pressure at the flowmeter was measured from CP-6 and the temperature from CT6. During the initial 150 seconds of the chilldown test, the fluid temperature was beyond the range of the temperature readout (100°R). During this initial phase of the chilldown test, the fluid temperature at the flowmeter was extrapolated based on the chill characteristics of the pump inlet fluid measured from CT-509. Shown on Table 2 are the flow rate computations.

4. Pump Inlet Condition

The fluid temperature measurements are made at various locations from the inlet flowmeter, KF-130, to the pump. Pressure and temperature (KT-130 and KP-130) are measured at the flowmeter. The fluid condition at the flowmeter was always two-phase except near the end of the chilldown test when the fluid was 100% vapor due to decrease in flow rate. Approximately 24 ft. downstream of the flowmeter, temperature sensor KT-4 indicated temperatures approximately

10°R greater than sensor KT-130 at the start of chilldown. This difference decreased to 5°R near the end of the test. Temperature sensor CT-3, located approximately 17 ft downstream of sensor KT-4, indicated temperatures approximately 2°R warmer than sensor KT-4. Temperature sensor CT-505 is located approximately 2 ft downstream of CT-3. CT-505 is located at the bottom of the line and was indicating temperature a few degrees below sensor CT-3. These temperature data indicate that temperature sensors KT-4 and CT-3 were not positioned at the bottom of the pipe line and temperature stratification exists in the line. The temperature data from sensor CT-505 indicate that the fluid in the pipe at this location (just downstream of valve C-4) was 100% vapor throughout the pump chilldown test (temperature above saturation based on measured pressure).

Approximately 7 ft downstream of CT-505 there are 4 temperature sensors placed circumferentially around the pipe starting at the top to 45°, 135°, 225° and 315° sectors. The two lower and one upper sensors readout temperatures below 45 and 54°R only. All three temperatures were off scale throughout the chilldown test. The other upper sensor indicates temperatures much hotter than measured from all other sensors in the line. The transient temperature measured from this sensor during the chilldown test is shown on Figure 2.

On a later chilldown test (December 22) the range of one of the lower sensor readouts (CT-508) was increased to 550°R. The differential temperature reading between the lower (CT-508) and the upper (CT-509) sensors was approximately 50°R during the chilldown test. These readings indicate a temperature stratification of 50°R in 70% of the 10 inch pipe diameter.

5. Pump Outlet Condition

The pump outlet temperature was measured by CT-542 located a few in. from the pump discharge. Since this measurement is made in a vertical pipe line, the measured temperature should be close to the mixed mean temperature. The readout was limited to 100°R; therefore, the pump outlet temperature was off-scale during the initial 100 seconds of the test.

Approximately 24 ft downstream of the pump discharge, temperature sensor CT-6 indicated temperatures approximately 10-20°R hotter than at the pump discharge. The readout for this sensor was also limited to 100°R and was greater than this value for the first 150 seconds of the chilldown test.

Based on these temperature data, the temperature rate of change at 100°R was very slow; therefore, the rapid temperature drop from 500°R (initial temperature) to approximately 200°R occurred very early in the test.

C. ANALYTICAL PUMP MODEL

1. Computational Method

There are several transient thermal analyzer computer codes available, but only the CINDA-3G (Reference 2) program has the capability of performing the computations necessary for this combined heat-transfer and fluid-flow problem. In CINDA, the computation of the heat transfer coefficients, vapor qualities, enthalpies, pressures and flow rates can be performed between each thermal transient computation of the solid nodes.

Several CINDA subroutines were written to perform the above computations and to use the National Bureau of Standards (NBS) hydrogen properties. The present program can handle a tank pressure and power chilldown case in a single computer run. From the pressure chill case, the program is able to switch to a power chill case at a specified time.

The thermal analysis was separated into regions--solid diffusion nodes and fluid nodes. When the temperatures of the solid diffusion nodes are being computed, the fluid nodes are treated as the boundary condition. The capacitance of the diffusion nodes and the conductance between these nodes are evaluated as functions of temperature during each iteration.

The temperature change rate of each solid node is computed by summing the total heat input from its adjoining solid or fluid nodes and dividing by its capacitance. The new temperature at each time step is computed explicitly by adding to the old temperature the product of the temperature change rate and the computing time step as follows:

$$Tn = To + \frac{G(Ta - To)}{C} \Delta\Theta$$

where:

Tn = new temperature, °R

Ta = temperature of connecting nodes, °R

To = old temperature, °R

G = conductance, Btu/sec-°R

C = capacitance, Btu/°R

$\Delta\Theta$ = computing time step, sec

The heat lost by the solid nodes is the summation of the heat convected to the fluid

$$Q = hA(T_S - T_F)$$

where

T_S = solid node temperature

T_F = fluid temperature

hA = film conductance

The fluid node conditions are computed based on a quasi-steady state solution. The heat gained from each solid node is computed assuming the solid nodes as boundary condition. The enthalpy of the fluid is computed assuming a saturated liquid condition at the inlet to the pump inlet line (PIL). At each fluid node, the energy gained from the solid is added to the upstream fluid node enthalpy. The fluid temperature and quality are determined from the NBS tables as a function of pressure and enthalpy (which is a function of temperature).

A subroutine was written to perform the iterative computation to determine enthalpy and temperature of the fluid nodes. At a fluid mixing node, where flow from two branches combine into one, the enthalpy value of the previous iteration is used for the initial condition of the secondary branch (fluid node

number greater than the mixing node number). If the difference between the new enthalpy value of this secondary branch node and the old exceeds a specified error limit, the whole fluid node computation for this time step is repeated using the new enthalpy value. A heat balance between the solid node and the fluid node computations is maintained, since a common set of solid node and fluid node temperatures and film conductance values are used for both computations.

2. Heat Transfer

The heat transfer characteristics from the solid to the fluid was separated into four distinct regimes: (a) laminar single phase, (b) turbulent single phase, (c) laminar two-phase, and (d) turbulent two-phase.

In the laminar single phase regime, the constant wall temperature forced laminar flow convection correlation given in Reference 3 was used

$$Nu = 3.65$$

where:

Nu = Nusselt number, $\frac{hD_h}{K}$

h = heat transfer coefficient, Btu/hr-ft^2-°R

D_h = hydraulic diameter, ft

K = thermal conductivity, Btu/hr-ft-°R

This correlation is valid for developed flow conditions (large L/D ratio). At smaller L/D ratios or near entrance of a passage, the heat transfer coefficient will be larger. Entrance effects were neglected since the L/D ratio of the coolant passages in general are large.

The Dittus-Boelter correlation (Reference 4) was used in the turbulent single phase regime. The heat transfer coefficient for this regime was computed as follows:

$$h = .023\ (CH)\ \frac{\dot{w}^{.8}}{D_h{}^{.2} A^{.8}}$$

where: $CH = K^{.6}(Cp/\mu)^{.4}$

Cp = specific heat, Btu/lb-°R

μ = viscosity, lb/hr/ft

$\dot{w}$ = flow rate, lb/hr

A = flow area, ft^2

The CH parameter was determined as a function of temperature and pressure from a table prepared from NBS hydrogen properties.

In the laminar two-phase regime, the film pool boiling correlation from Reference 5 was used. The following equation was fitted from the flat plate data of Figure 2.7 of Reference 5:

$$h = 48. + \frac{0.133}{D_h}$$

The heat transfer correlation in the unstable transition region was not included since its effect is not felt until the film temperature difference becomes less than 40°R. Nucleate boiling does not occur until the film temperature difference is below 10°R; therefore, it was also neglected.

In the turbulent two-phase flow regime, the forced convection film boiling correlation given in Reference 6 was used.

$$h_{2\phi} = h_{1\phi}\left[\frac{\frac{x}{\rho_b} + \frac{1-x}{\rho_L}}{\frac{x}{\rho_f} + \frac{1-x}{\rho_L}}\right]^{.8}\left[\frac{\left[\frac{Cp}{\mu_K}\right]_f^{.4} K_f}{\left[\frac{Cp}{\mu_K}\right]_b^{.4} K_b}\right]\frac{Nu\ exp}{Nu_{calc.}}$$

where:

$h_{2\phi}$ = 2-phase forced convection heat transfer coefficient, Btu/hr-ft^2-°R

$h_{1\phi}$ = vapor heat transfer coefficient at saturation conditions, Btu/hr-ft^2-°R

K_f = thermal conductivity at film temperature, Btu/hr-ft-°R

K_b = thermal conductivity at bulk temperature

x = vapor quality, weight fraction

ρ_b = bulk vapor density, lb/ft^3

ρ_L = liquid density, lb/ft^3

ρ_f = vapor density at the film temperature, lb/ft^3

The Dittus-Boelter heat transfer coefficient evaluated at the saturated vapor condition is used for $h_{1\phi}$ in the above equation. The first bracketed term is the ratio of the average fluid densities evaluated at the film and bulk temperatures. The second term is the ratio of the vapor physical properties evaluated at the film and bulk temperatures. The last term is the empirical Nusselt number ratio shown on Figure 4, replotted from page 447 of Reference 6, as a function of vapor quality. The data scatter of this parameter is approximately +100% and -50% of the mean. The mean value was used in this analysis.

The effect of the contact thermal resistance was neglected since almost all mating surfaces must be sufficiently tight to minimize vibrations. As a point of reference, it might be noted that one mil of hydrogen gas gap corresponds to a contact conductance of approximately 500 Btu/hr-ft^2-°R, which in turn corresponds to an additional thickness of only 0.05 inch of titanium or 0.026 inch of stainless steel. At room temperature, the radial clearance between the stainless steel bearing race and the titanium rotor parts can be several mils, and at cryogenic temperatures, these gaps would close because the thermal expansion coefficient of titanium is approximately half that of stainless steel. Therefore the contact thermal resistances are the greater for a warm pump.

3. Fluid Flow

The TPA model flow chart is shown on Figure 5. The hydrogen flow rates through the various passages in the TPA were computed assuming all the available pressure drop occurred at a single restriction in each passage. These restrictions are the labyrinth seals and bearing feed line orifices. The flow coefficients across these restrictors are determined from the TPA design group, and the flow rates were computed as follows:

$$\dot{w} = \sqrt{\Delta P \times G \times \bar{\rho}}$$

where: $\dot{w}$ = fluid flow rate, lb/sec

ΔP = pressure drop, psi

$G = 24g(AC)^2$, flow coefficient, in^5/sec^2

A = flow area in^2

C = orifice flow coefficient

$\bar{\rho}$ = average homogeneous fluid density downstream of the restriction, lb/in^3

Although this equation is for an incompressible fluid, its approximation of isentropic gas flow through an orifice was good for this application since the downstream fluid density is used. The compressible flow equation can be written as follows (Reference 7):

$$w = Y \sqrt{\frac{\Delta P}{V_1} G}$$

where Y is the net expansion factor and V_1 is the specific volume of the upstream fluid (in^3/lb). The two flow equations are identical if

$$\frac{Y}{\sqrt{V_1}} = \sqrt{\rho_{out}}$$

Using the net expansion factors for an orifice given in Reference 7 for orifice diameter ratios of 0.2 to 0.8, values for the parameter $Y\sqrt{\frac{\rho_{in}}{\rho_{out}}}$ were computed to be close to unity. For single phase, gas flow, the density ratio was computed as a function of pressure as follows:

$$P_1 V_1^{1.4} = P_2 V_2^{1.4} \text{ or } \frac{\rho_1}{\rho_2} = \left[\frac{P_1}{P_2}\right]^{1/1.4}$$

For the two-phase fluid case, it was assumed that the fluid is homogeneous with an average density computed as follows:

$$\bar{\rho} = \frac{1}{\frac{X}{\rho_v} + \frac{1-X}{\rho_L}}$$

where ρ_L = liquid density, lb/in^3

ρ_v = vapor density, lb/in^3

4. Model Definition

The single stage test pump configuration used to develop the finite difference model was AGC Drawing No. 1139300. This model has 520 solid nodes, 266 surface nodes and 133 fluid nodes in a two-dimensional axisymmetric coordinate system. The grid of this model is shown on Figure 5. The pump inducer, impeller blades and the diffuser vanes were included in this model as fractional mass nodes. The pump inlet line to Valve C-4 was also modeled.

Since this pump model was developed prior to the actual chill-down testing, the pump model was modified to best use the test data available to perform the data simulation analyses. Because the hydrogen condition at Valve C-4 was two-phase and the quality was not known, it was assumed that the fluid condition

at the pump inlet was always gas. This assumption was based on the temperature data taken between the flow conditioner and the pump inlet bellows. The bearing coolant flow rate was determined by the measured pressure drop at the filter rather than by the labyrinth seal configuration.

The original model had the capability of simulating a powered chilldown case (pump rotated at some reduced speed). Powered chilldown tests were not performed. In the pressure chilldown case, many of the fluid nodes are treated as stagnant gas pockets.

5. Condition Analyzed

The objective of this analysis is to predict the measured temperature response of the pump during the pump chilldown test. The pump inlet fluid condition (enthalpy), fluid flow rate through the pump and the pump initial temperature are required as input to the analytical computer model of the pump.

The fluid flow rate data from the pump outlet flowmeter CF-6 was used. The flow rate values computed on Table 2 were modified slightly because the flowmeter is approximately 24 ft from the pump discharge and some lag in flow response can be expected. The data indicated that steady flow rate value at the outlet flowmeter was reached in 20 seconds. It was assumed in this analyses that the pump steady flow rate value was reached in 5 seconds.

The initial temperature of the pump was assumed to be a uniform 500°R. All of the temperature sensors in the pump metal and bearing coolant passage indicated between 490 and 505°R.

The pump inlet fluid condition was based on the pump inlet full range temperature sensor, CT-509, and the pump outlet temperature sensor CT-542. Because CT-542 is located in a vertical pipe line, it probably senses fluid temperature near the mix mean value. Since the pump inlet temperature must be cooler than the outlet, the mean pump inlet temperature was assumed to be an arbitrary 20-30°R lower than the measured pump outlet temperature. This temperature placed the fluid in the super-heated vapor region. In the initial part of the chilldown test where CT-542 was off-scale, the pump inlet fluid temperature was extrapolated following

the characteristic curve of the pump inlet temperature data from CT-509. The reason CT-509 data could not be used directly is that it is a measure of a temperature in the upper region of a horizontal pipe. Due to temperature stratification in the pipe line, CT-509 only senses the temperature of the fluid in the upper portion of the pipe and not the mixed mean temperature. Shown on Table 3 are the input parameters used for the nominal case.

IV. RESULTS

A. NOMINAL CASE ANALYSIS

The pump thermal transient response computed by the pump model for the nominal input case is shown on Figure 6. The temperature transient measured in the pump housing decayed much faster than computed from the model. The pump housing temperature sensor locations are shown on Figure 3. These sensors are positioned in the housing 0.2 to 0.4 in. from the fluid in front of the impeller blade near the exit. In the pump model, it was assumed that the fluid in front of the impeller adjacent to the housing in front of the temperature sensor was stagnant. The flow area through the pump impeller is approximately 1000 times greater than through the impeller forward labyrinth seal. The impeller was locked in place to prevent free wheeling during the chilldown.

The test data indicated a large temperature difference of approximately 80°R between the sensors located 0.2 and 0.4 in. from the surface. The analytical model predicted a temperature difference of only 20°R. The large temperature gradient is in the axial direction toward the pump diffuser which is in contact with flowing coolant. Thus the test data indicate a large gradient axially toward the stagnant gap between the housing and impeller; but the analytical model predicts the temperature gradient is radially outward toward the diffuser.

The gap between the impeller and the housing may be sufficient to form eddy currents in the region assumed to be stagnant gas. This current could increase the effective thermal conduction from the housing to the front impeller shroud.

This same flow discontinuity between the impeller discharge and diffuser inlet could increase the convective heat transfer coefficient at the diffuser inlet region of the housing. At the entrance region of a constant configuration passage, the convective heat transfer coefficient starts at infinity and approaches the steady-state developed flow value.

Even though the measured pump inlet and outlet temperature sensors indicate superheated vapor, some liquid droplets may be carried along with the vapor and have the characteristics of two-phase hydrogen for convective heat transfer consideration. The two-phase convective heat transfer correlation predicts a much higher value at very high vapor quality than for 100% vapor condition.

The hydrogen flow rate through the pump may be in error by as much as 50% since gas, not liquid, was passing through the flowmeter and because the temperature data were extrapolated above 54°R. A 50% increase in flow rate has an effect of increasing the convective heat transfer coefficient by 38%.

Thus there are at least four phenomenon which might explain the faster chilldown of the pump than predicted by the analytical model.

B. PARAMETRIC ANALYSIS

The only way that the pump can chill down faster than computed in the nominal case is to increase the convective heat transfer coefficient. This can be done by increasing the flow rate and/or multiplying the computed coefficient by a factor greater than unity to account for the high heat transfer coefficient at entrance region (or discontinuities). Shown on Figure 7 is the computed pump transient response with 50% increase in flow rate and a factor of two on computed heat transfer coefficient. This computed temperature decay is still much slower than the experimental data. On the next analyses, the computed heat transfer coefficient was increased by a factor of four with the flow rate remaining at 1.5 times nominal. The temperature transient computed from this analyses is shown on Figure 8.

The fluid inlet temperature which is a function of time was the same in all three computer analyses. The computed pump outlet temperature from all three analyses were all close to the measured value.

V. REFERENCES

1. Memo N8300R:71-060, F. X. Andrews and T. Nishioka, dated 24 May 1971, Subject: Test Plan LH_2 Pump Component Development Testing in the Electric Pump Room at Test Cell "C"

2. J. D. Gaski, D. R. Lewis, L. R. Thompson, "Chrysler Improved Numerical Differencing Analyzer for 3rd Generation Computers", CINDA-3G, October 20, 1967, Technical Note #TN-AP-67-287

3. E. R. G. Eckert and R. M. Drake, "Heat and Mass Transfer", McGraw-Hill Book Company, Inc., 1959

4. W. H. McAdams, Heat Transmission, New York, McGraw-Hill, 1954, p 219

5. "Boiling Heat Transfer for Oxygen, Nitrogen and Hydrogen Helium", NBS Technical Note No. 317, September 20, 1965

6. J. A. Clark, "Advances in Heat Transfer 1968", Academic Press, 1968

7. "Flow of Fluid Through Valves, Fitting and Pipe", Crane Industrial Products Group, 4100 S. Kedzie Ave., Chicago 32, Illinois, Technical Paper #411, 1957

TABLE 1

INSTRUMENTATION SUMMARY

Channel	Range	
CT-700	35-590°R	Pump housing, θ = 288°, 0.2 in. from fluid
CT-701	35-590°R	" " , θ = 270°, 0.3 in. " "
CT-702	35-590°R	" " , θ = 252°, 0.4 in. " "
CT-703	35-590°R	Pump bearing fluid between bearings
CT-704	35-100°R	Pump forward bearing, θ = 0°
CT-705	35-100°R	Pump forward bearing, θ = 180°
CT-706	35-100°R	Pump aft bearing, θ = 135°
CT-707	35-100°R	" " " , θ = 315°
KT-130	35-54°R	KF-130 Flowmeter inlet
CT-3	35-590°R	Inlet line
CT-505	35-54°R	Flow conditioner inlet
CT-506	35-45°R	Pump inlet, θ = 45°
CT-507	35-54°R	" " , θ = 135°
CT-508	35-54°R	" " , θ = 225°
CT-509	35-590°R	" " , θ = 315°
CT-542	35-100°R	Pump discharge
CT-6	35-100°R	Flowmeter, pump discharge CF-6
CP-702	0-750 psi	Differential pressure, bearing feed orifice #1
CP-730	0-750 psi	" " " " " #2
KP-130	0-100 psig	Chill flowmeter inlet KF-130
KP-3	0-100 psig	Pump inlet line
CP-541	0-1000 psig	Pump discharge line
CF-6	0-100 lb/sec	Pump discharge flow rate
KF-130	0-5 lb/sec	Chilldown flow rate

TABLE 2

PUMP CHILLDOWN FLOW RATE CALCULATION

December 10 Data

Pump Outlet Pressure = 14 psia

	Pump Outlet Flowmeter Data		Pump Flow Rate Calculation		
θ sec	Indicated Flowrate CF-6 (1) lb/sec	Temperature CT-6 °R	Density ρ (3) lb/ft^3	Density Ratio ρ/4.3	Flow Rate ẇ(calc) (4) lb/sec
0	0	300 (2)	.009		0
10	38	220 (2)	.013	.00303	.145
20	52	160 (2)	.017	.00396	.206
30	52	144 (2)	.020	.00466	.243
40	50	136 (2)	.023	.00537	.267
60	46	127 (2)	.025	.00582	.267
80	45	120 (2)	.026	.00605	.266
100	40	114 (2)	.027	.00630	.252
120	37	109 (2)	.028	.0067	.24
140	35	104 (2)	.029	.0067	.234
160	33	98	.029	.0067	.221
180	32	94	.030	.0070	.224
200	29	87	.032	.0074	.214
220	27	82	.035	.0082	.220
240	26	79	.035	.0082	.213
260	26	78	.035	.0082	.213
280	24	81	.035	.0082	.196
300	22	88	.032	.0074	.162

(1) CF-6 calibrated based on ρ = 4.3 lb/sec

(2) Estimated value based on CT-507 data

(3) $\rho = \frac{12\rho}{386T}$, lb/ft^3

(4) w = (CF-6) * ρ/4.3

TABLE 3

INPUT PARAMETERS

Nominal Case

Initial Pump Temperature = 500°R

Pump Flow Rate		Pump Inlet Condition		
θ sec	$\dot{w}$ lb/sec	θ sec	Enthalpy Btu/lb	Temp °R
0	.1	0	720.	250.
5.	.26	10.	405.	160.
200.	.26	20.	295.	120.
250.	.24	30.	245.	100.
310.	.20	50.	220.	90.
		100.	180.	75.
		150.	155.	65.
		200.	140.	60.
		250.	130.	55.
		310.	140.	60.

SCHEMATIC, PUMP TEST, ELECTRIC DRIVE, TEST CELL 'C'
FACILITY INSTRUMENTION

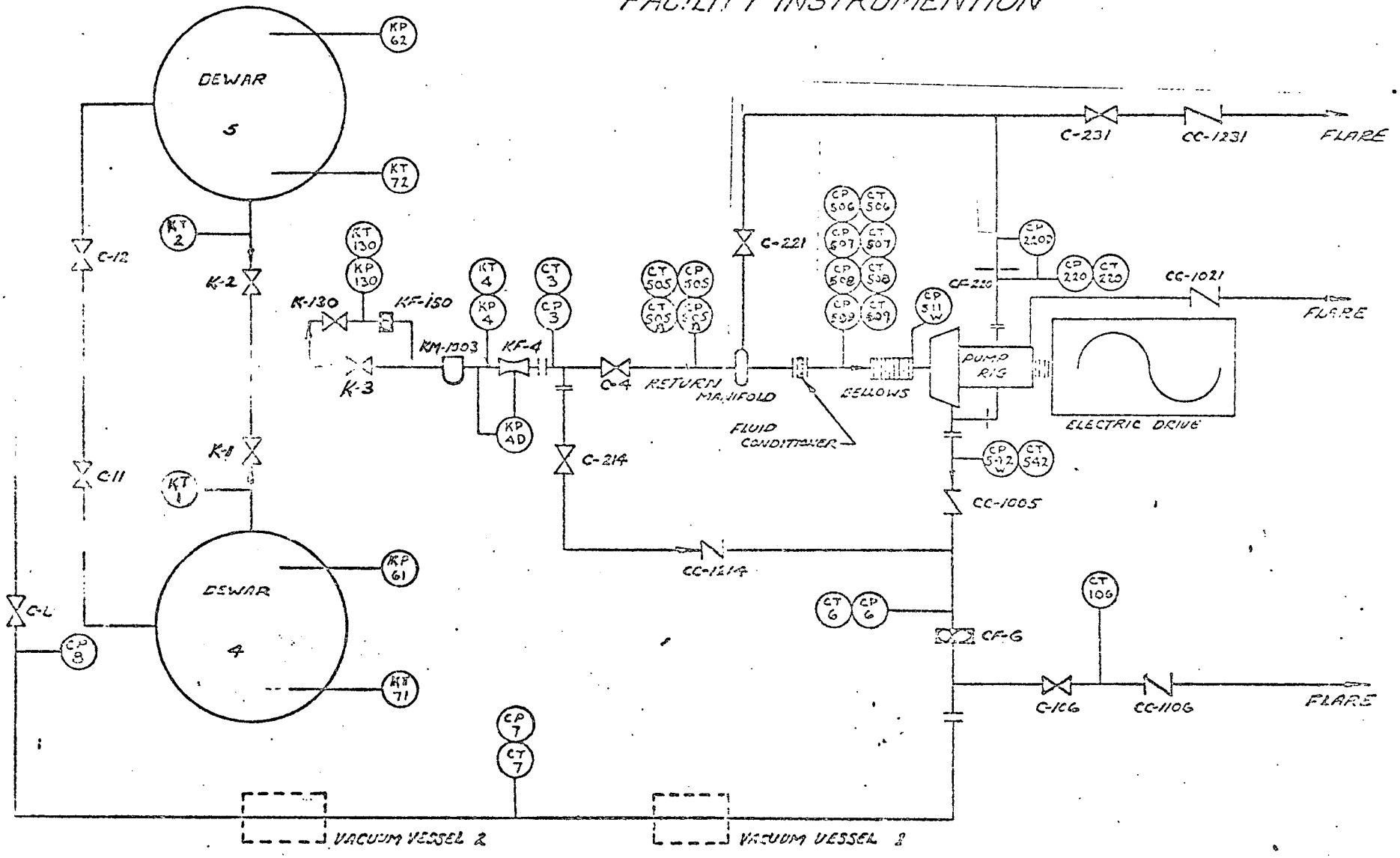

FIGURE 2

L. A. Kamura
7 June 1972

R81108:72-033
Page 22

PUMP HOUSING TEMPERATURE

SENSOR INSTALLATION

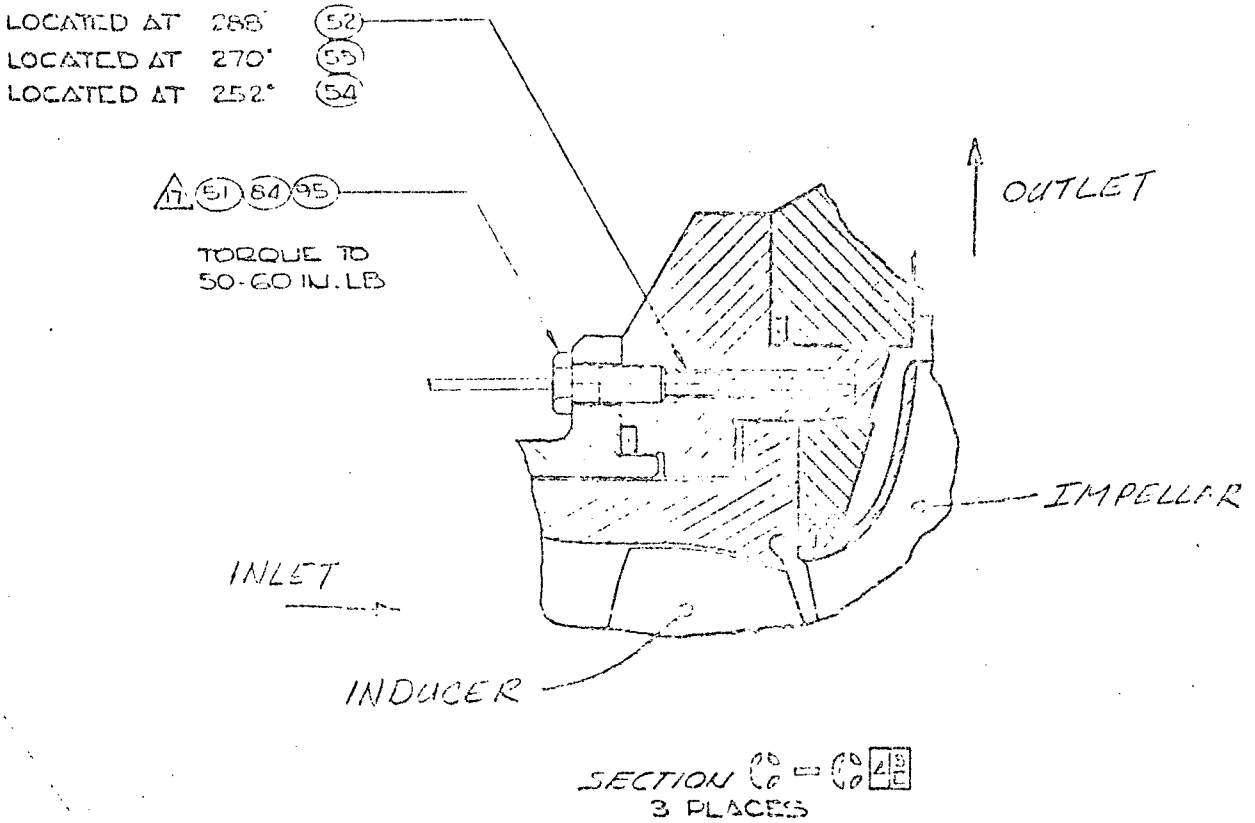

FIGURE 3

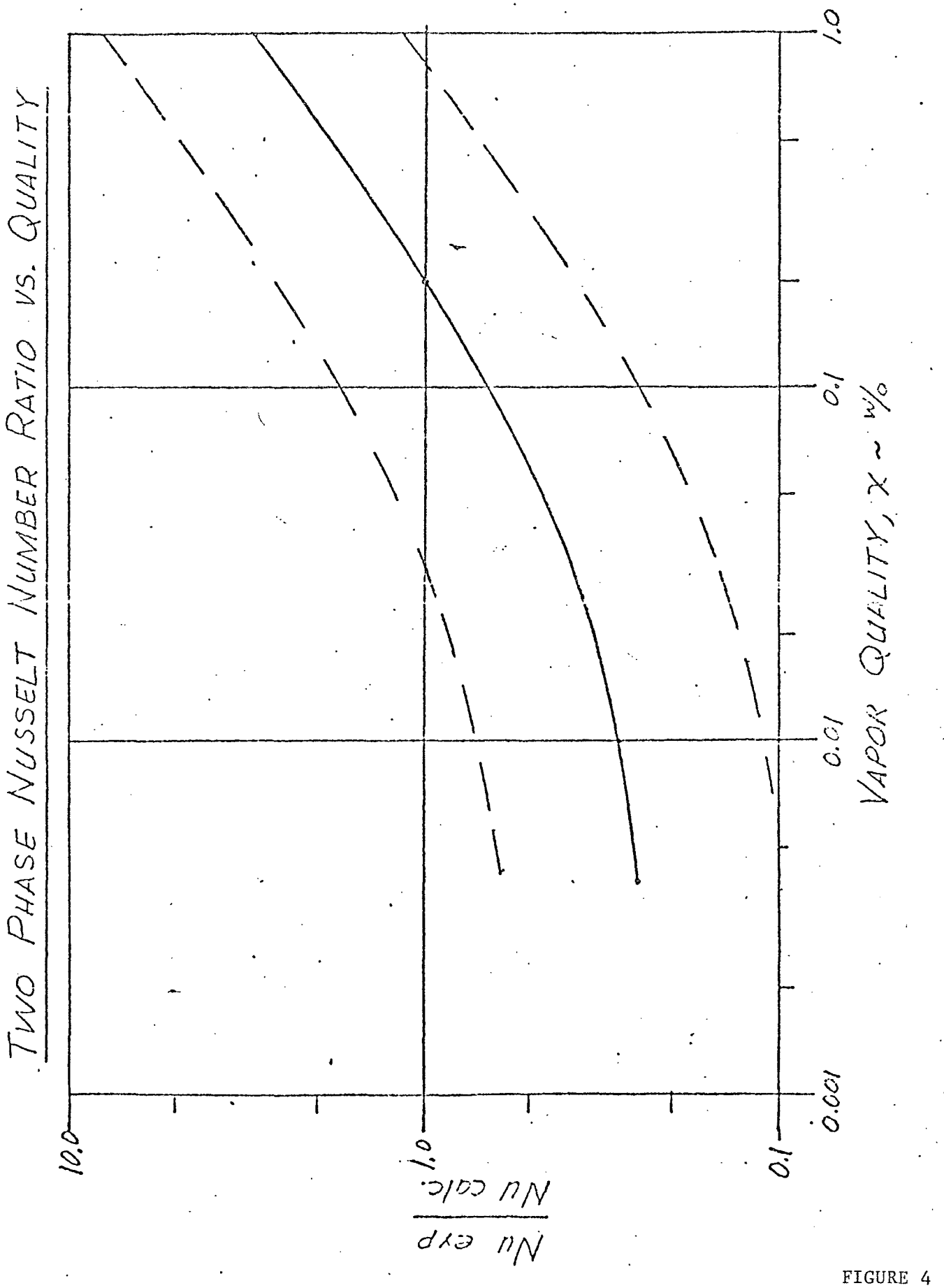
TWO PHASE NUSSELT NUMBER RATIO VS. QUALITY
Nu exp / Nu calc.
10.0
1.0
0.1
1.0
0.1
0.01
0.001
VAPOR QUALITY, x ~ w/o
REF. ADVANCES IN HEAT TRANSFER 1968, PG 447

FIGURE 4

SINGLE STAGE PUMP FINITE DIFFERENCE MODEL

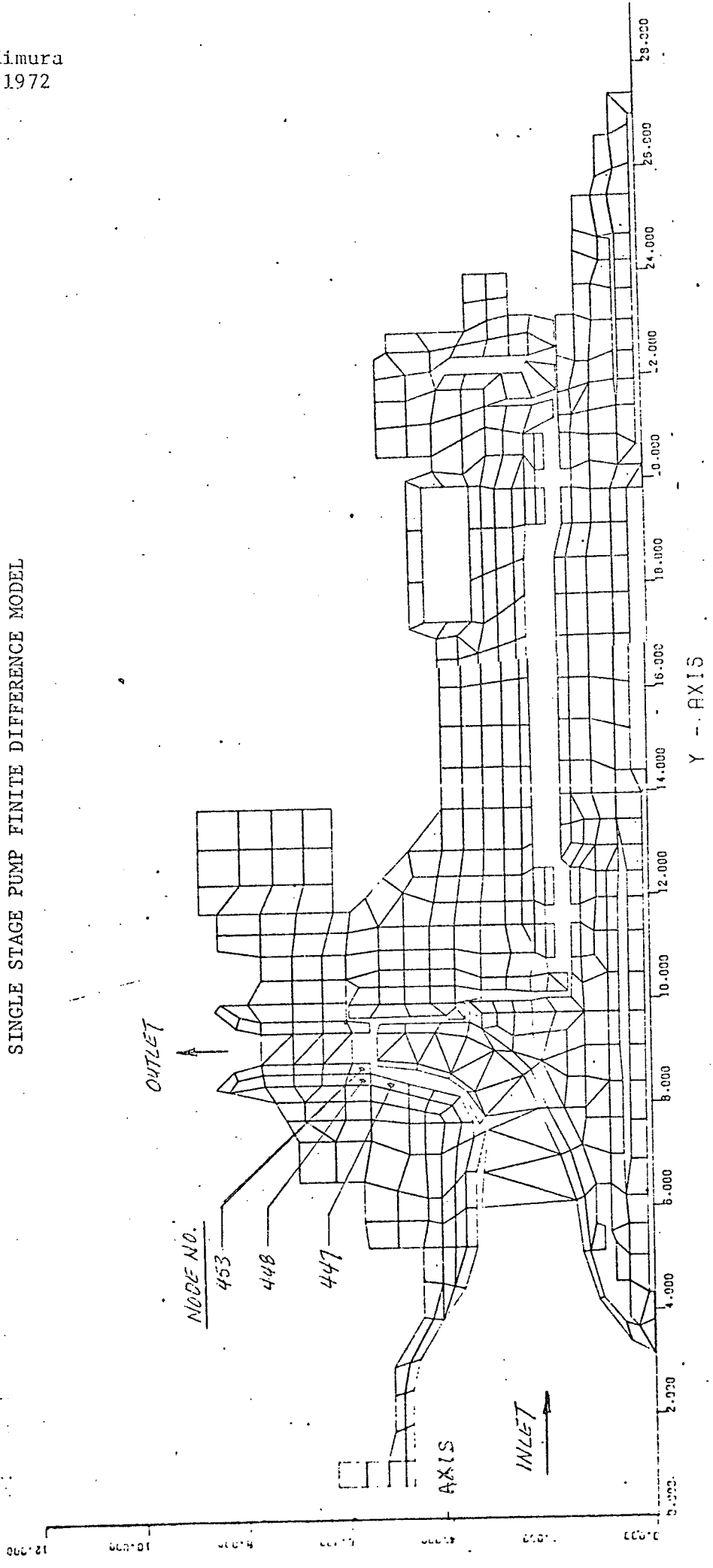

FIGURE 5

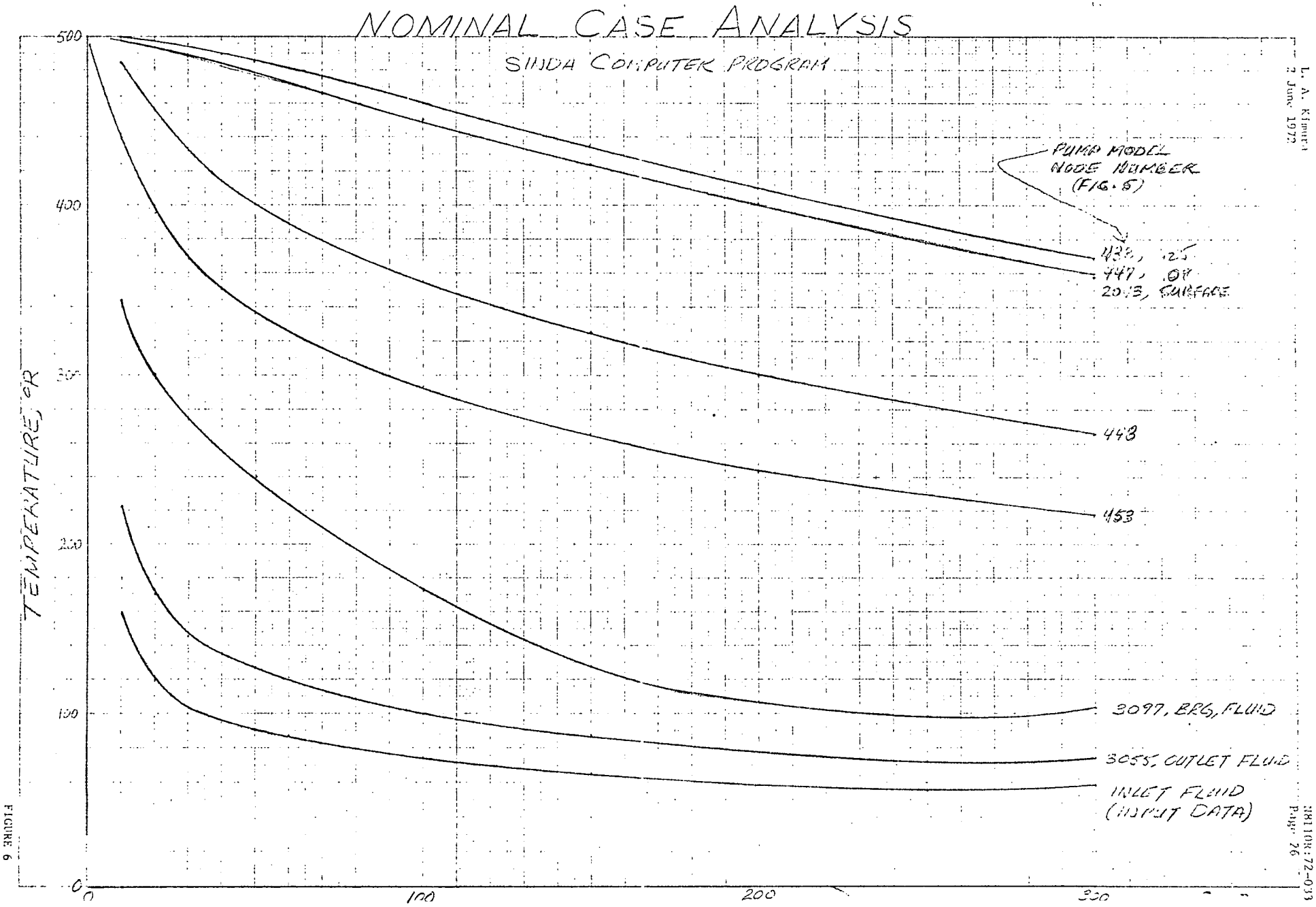

FIGURE 6

L. A. Kimmel
2 June 1972

BELLCOMM, INC.
Page 26

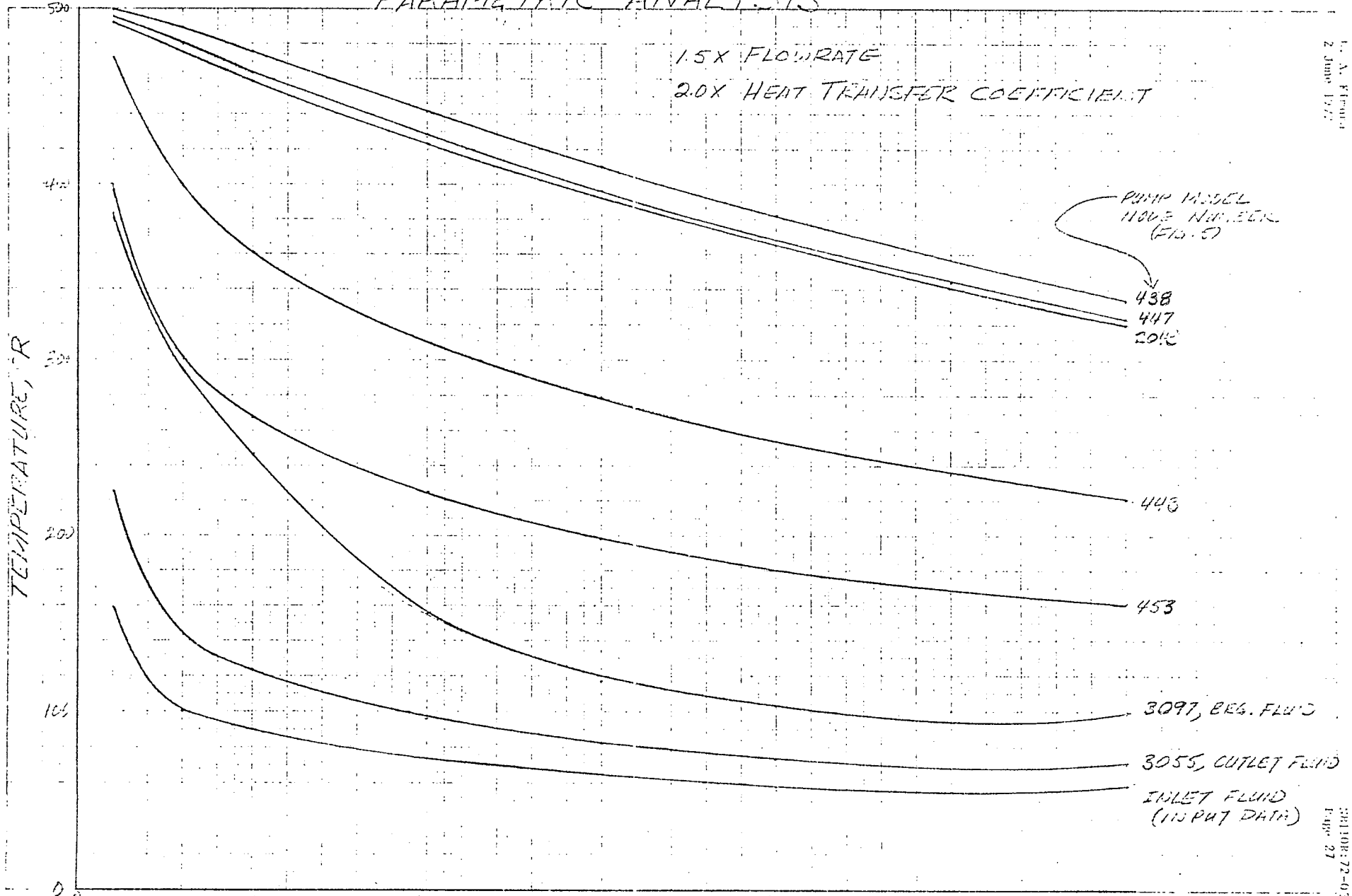
PARAMETRIC ANALYSIS
1.5X FLOWRATE
2.0X HEAT TRANSFER COEFFICIENT
TEMPERATURE, °R
PUMP MODEL NUMBER (FIG. 5)
438
447
453
3097, REG. FLUID
3055, OUTLET FLUID
INLET FLUID (INPUT DATA)
0
100
200

FIGURE 7

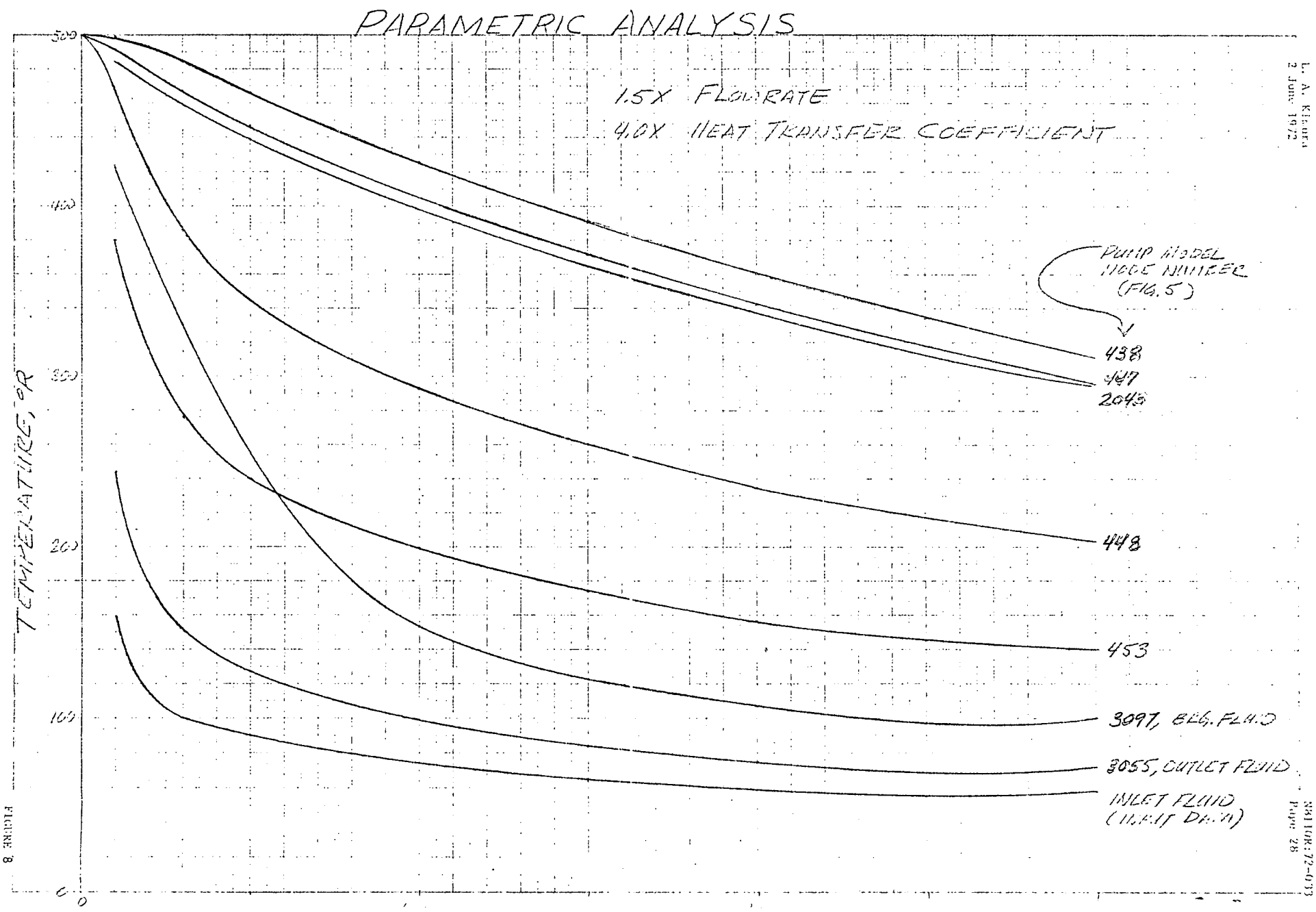

FIGURE 8

L. A. Kleucz
2 June 1972

SR110R-72-013
Page 28